Eur Radiol (2013) 23:702–711
DOI 10.1007/s00330-012-2642-8

CHEST

Morphological changes of the thoracic duct and accessory lymphatic channels in patients with chylothorax: detection with unenhanced magnetic resonance imaging

De-xin Yu · Xiang-xing Ma · Qing Wang · Yang Zhang · Chuan-fu Li

Received: 20 April 2012 / Revised: 19 July 2012 / Accepted: 6 August 2012 / Published online: 14 September 2012

Abstract
Objectives To characterise the imaging findings of patients with chylothorax and to identify the leak site using unenhanced MRI.
Methods Seven patients with chylothorax and 30 healthy individuals (as the control group) underwent three-dimensional heavily and routine T2-weighted MRI. Morphological changes and diameters of the thoracic duct, chyloma display, and some dilated accessory lymph channels were evaluated and measured. The differences between patients and the control group were compared. The leak sites of the thoracic duct and parietal pleura were also identified.
Results The patients had a higher display rate of the entire thoracic duct and some accessory lymphatic channels, enlarged diameters and tortuous configuration of the thoracic duct, and existence of chylomas compared with the control group ($P<0.05$). Seven leaks of the thoracic duct in five patients and five leaks of the parietal pleura in four patients were identified. Close relationships between the leak of thoracic duct and the chylomas or the meshworks of tiny lymphatics were found ($P<0.05$).
Conclusion Unenhanced MRI appears reliable in the detection of morphological changes of thoracic lymphatics and in the identification of chyloma and leak sites in patients with chylothorax, which helps appropriate treatment planning and follow-up.
Key Points
- *Unenhanced MRI can display the abnormal imaging findings in patients with chylothorax.*
- *MRI can reveal the leak sites of the thoracic duct and parietal pleura.*
- *MRI provides a useful tool for appropriate treatment planning and follow-up.*

Keywords Chylothorax · Thoracic duct · Chyle leak · Chyloma · Magnetic resonance imaging

D.-x. Yu · X.-x. Ma (✉) · Q. Wang · Y. Zhang · C.-f. Li
Department of Radiology, Qilu Hospital of Shandong University, 107 Wenhuaxi Road,
Ji'nan City, Shandong Province, China 250012
e-mail: maxx2006@yahoo.cn

D.-x. Yu
e-mail: ydx0330@sina.com

Q. Wang
e-mail: wangqing0534@yahoo.com.cn

Y. Zhang
e-mail: drzhy001@163.com

C.-f. Li
e-mail: chuanfu.li@yahoo.cn

Introduction

Chylothorax is a rare entity with obscure aetiology and is infrequently encountered by most physicians. It is characterised by the accumulation of fluid that contains cholesterol and triglyceride in the pleural cavity, which may result from the rupture and obstruction of the thoracic duct or its branches [1–3]. Thus, the visualisation of the thoracic duct and the accessory lymph channels and the identification of the leak sites are essential to elucidate the cause of chylothrax and may assist in selecting the optimal therapy for each patient and in avoiding thoracic duct injury during surgery. However, the lymphatic duct cannot be easily observed owing to its small size [4, 5]. Although the most common imaging techniques for the lymphatic channels are scintigraphy and radiograph lymphography [6], these techniques have a number of drawbacks such as contrast material discomfort, radiation exposure, and lower tissue resolution [7]. The thoracic duct has been visualised using

unenhanced MR imaging (MRI) with a highly fluid-sensitive sequence that has a higher display rate than radiograph lymphography [8–12]. We also previously described a suitable method for thoracic duct visualisation using heavily T2-weighted imaging (T2WI) [13]. Aside from anatomical literature, the morphological changes in the lymphatic ducts caused by several abdominal disorders have been previously reported, such as liver cirrhosis, malignancy, and biliary obstruction [9, 10]. Thus far, no study has reported on the morphological changes in patients with chylothorax using MRI. The ability of unenhanced MRI to visualise the morphological changes in the thoracic duct and in the accessory lymph channels in patients with chylothorax must be investigated. The present study aims to characterise the abnormal MR findings of the patients with chylothorax compared with a control group and to identify the leak site of the thoracic duct.

Materials and methods

Patients

From September 2008 to August 2011, seven Chinese patients of both genders (5 women and 2 men, ranging from 23 years to 58 years, mean age of 38.4 years) with suspected chylothorax were referred to our hospital for further diagnosis and treatment. During this period, 30 healthy subjects (12 women and 18 men, ranging from 16 years to 67 years, mean age of 48.4 years) were chosen as the control group from those who underwent physical examination in our hospital. All individuals in the control group were proved to have no disease based on the clinical examination results and were enrolled in the study before undergoing MRI. The diagnosis of chylothorax was confirmed by chemical analysis of the milky fluid obtained by percutaneous needle aspiration with the presence of chylomicrons and a triglyceride level >4.52 mmol/L. Among these patients, the causes were identified as traumatic with definite history in two patients, lung lymphangioleiomyomatosis proven by thoracic high-resolution CT and lung fine-needle biopsy in two, non-Hodgkin's lymphoma in one, and uncertain cause in two. Two patients with traumatic cause underwent the MR imaging during the 3rd and 5th day after the injury. The pleural effusion before the drainage procedure was quantified using an ultrasound measurement method presented by Eibenberger et al [14]. The volume of pleural effusion was classified into three grades as follows: less (≤380 ml with an effusion width ≤20 mm), moderate (380 ml to 1,000 ml with an effusion width from 20 mm to 40 mm), and severe (≥1,000 ml with an effusion width ≥40 mm) according to the maximum width of the fluid lamella along the lateral chest wall at ultrasound during maximum inspiration with the patient completely supine. The ethics committee in our hospital approved the study, and written informed consent was obtained from all patients and individuals from the control group for MRI and other medical procedures.

MR imaging

All examinations were performed using 3.0-T MR (Signa Excite, GE Healthcare, Milwaukee, WI, USA) with an eight-channel torso phased-array coil. The three-dimensional (3D) heavily T2WI and axial and coronal fat-saturated T2WI (FS-T2WI) were performed with fast spin-echo sequences. During this period, respiratory gating was performed, and TR and TE were automatically ranged using the software according to the respiratory rate and the patient's body volume. The imaging parameters of FS-T2WI were as follows: TR range/TE range, 4,000 ms to 8,000 ms/70 ms–110 ms; section thickness, 4 mm; intersection gap, 1.5 mm; field of view (FOV), 360 mm to 380 mm; matrix size, 320×224 pixels; number of excitations, 2; acquisition time range, 4 min to 7 min. The imaging parameters for the 3D heavily T2-weighted imaging were: TR range/TE range, 2,000 ms to 4,500 ms/550 ms to 750 ms; section thickness, 1.5 mm; no intersection gap; FOV, 380 mm to 460 mm; matrix size, 320×256 pixels; number of excitations, 2; acquisition time range, 5 min to 12 min. The craniocaudal anatomical boundary was between the thorax entrance and the lower pole of the kidney, whereas the anteroposterior range was from the vertebral to the abdominal wall. Prior to the examination, all subjects were subjected to at least 4 h of fasting. For four patients with pleural effusion of more than 380 ml, the effusion was drained 2 h prior to the MRI.

Observation of image

A maximum intensity projection (MIP) reconstruction of the resource images of the 3D highly fluid-sensitive sequence was obtained at a workstation (advantage Windows, version 4.2). This sequence can emphasise signals from the liquid fraction and can suppress other signals because of a long echo time. Therefore, the 3D MIP images provide an excellent view with a high spatial resolution used to evaluate the configuration of the thoracic duct and the accessory lymph channels in any orientation. Several fluid-containing hyperintense structures, such as the stomach, gallbladder, hepatic duct, common bile duct, pancreatic duct, renal pelvis, part of the ureter, and spinal canal, which may overlap with the thoracic duct and the accessory lymph channels, were cut out from MIP images to decrease the interference of the water in other organs in the visualisation of the thoracic duct and the accessory lymph channels. The entire view and tortuous configuration of the thoracic duct, chyloma as well as some dilated accessory lymph channels were observed based on the MIP images. The chyloma was defined as a

cyst-like structure filled with chyle, which runs out from the thoracic duct or the lymphatics and locally accumulates in the posterior mediastinum until the mediastinal pleura ruptures [15]. The maximum anteroposterior and transverse diameters of the thoracic duct on the MIP image were then measured after magnifying the images. For the anatomical variation of the thoracic duct as double ducts, the maximum diameter was measured by adding the diameter of both parts. The observation and measurement in all subjects were performed by consensus between two experienced radiologists who were blind to the clinical details and diagnosis. The observation of the leak site in seven patients was also performed by the two radiologists. Every slice of the continuous images (the axial and coronal T2WI combined with the thin source images of the 3D heavily T2WI) was carefully reviewed to find the leak sites of the thoracic duct and of the parietal pleura.

Statistical analysis

Statistical analysis was carried out with the SPSS soft package 17, USA. The measured diameters were expressed as means ± SD. A two-tailed unpaired Student's *t* test with a confidence level of 95 % (unequal variances assumed) was used to compare the groups with respect to the diameters of the thoracic duct. The display differences in the thoracic duct, some accessory lymph channels, and chyloma between the patients and the individuals from the control group, and the relationships between the leak and other parameters evaluated, were analysed using the chi-squared test. A *P* value of less than 0.05 was considered statistically significant.

Results

Differences in imaging findings between the patients and the control group

Table 1 shows the differences in the display of the entire view and tortuous configuration of the thoracic duct, chylomas, and some dilated accessory lymph channels, and in the diameters of the thoracic duct between the patients and the individuals from the control group. The 3D-MIP images showed an entire view of the thoracic duct in five patients (Figs. 1, 2, 3 and 4), the lower two-thirds of the duct in two, and the tortuous configuration in four (Figs. 2 and 4) (Table 2). We also found that two patients had a variation with bilateral thoracic ducts (Fig. 2). By comparison, amongst the 30 individuals from the control group, an entire view of the thoracic duct was obtained in 5 subjects and the middle and/or lower duct in 25 with tortuous configuration in 3 and tubular duct in others. In addition, chylomas were found in six patients (85.7 %, 6/7), which had well-demarcated and cyst-like high signal near the lower and/or middle portion of the thoracic duct. Five of these patients had multiple chylomas surrounding the thoracic duct or thoracic aorta (Figs. 1c and 2) and one patient had a single chyloma on the right side of the aorta (Fig. 3b). However, no chyloma was found in the control group. Moreover, the 3D MIP images also demonstrated two kinds of the dilated accessory lymph channels (Table 2). The first was some meshworks of tiny lymphatics with hyperintensity lying along the vertebral or para-aortic region in the upper abdomen (Figs. 1a and b, 2a and b and 3a) in five patients and in six individuals from the control group. These meshworks connected the cisterna chyli via small lymph ducts or lymph trunks. The second was located in the left subclavian region that was connected to the terminal portion of the thoracic duct, but one patient had no chyloma and lymphatic meshworks in the para-aortic region (Fig. 4a). The statistical results revealed that the maximum transverse and anteroposterior diameters of the thoracic duct measured in patients (4.8±1.3 mm and 4.5±1.3 mm, respectively) were significantly greater than those of the control group (3.4±0.5 mm and 3.1±0.4 mm, respectively) (t=2.862, P=0.027; t=2.763, P=0.031). In addition, the display rates of the entire view and tortuous configuration of the duct, chyloma, and dilated lymph channels in the para-aortic region and in the left subclavian region in patients were higher than those of the control group (Fig. 5) (P<0.05).

Identification of the leak site

In this study, no leak site was revealed in a patient who had dilated and tortuous lymphatic channels in the left subclavian region but without chyloma and lymphatic meshworks in the para-aortic region (Fig. 4). Leaks from the thoracic duct to the chyloma and from the chyloma to the pleural cavity were identified based on the axial and coronary T2WI combined with the thin source images of the 3D heavily T2WI because of existence of the chylomas in most patients. Seven leak sites from the thoracic duct to chylomas were identified (Figs. 1c, 2c and d and 3b) in five patients, two of whom with bilateral thoracic ducts had a leak site in every duct and three of whom had one leak (Table 2). The leak site was difficult to identify in another patient because of the overlap with the neighbouring chyloma or pleural effusion. Five leak sites of the parietal pleura from the mediastinal chyloma to the pleural cavity were revealed in two patients with the leak site in the left side (Fig. 2c), one patient with the leak site in the right side (Fig. 3b), and one patient with two leak sites in the bilateral sides (Table 2). No leaks were observed in two patients with chylomas because of the overlapping or covering of more high signals of pleural effusion. Moreover, the leak sites of the thoracic duct were identified in five patients with chylomas or meshworks of tiny lymphatics. The relationship between the leak and the

Table 1 The differences in imaging findings between the patients with chylothorax and the control group

Groups	*n*	Thoracic duct				Chyloma	Dilated accessory lymph channels	
		Entire display	Tortuous duct	Transverse diameter (mm)	Anteroposterior diameter (mm)		Meshworks of tiny lymphatics	Lymphatics in left subclavian region
Patients	7	5 (71.4 %)	4 (57.1 %)	4.8±1.3	4.5±1.3	6 (85.7 %)	5 (71.4 %)	1 (14.3 %)
Controls	30	(16.67 %)	3 (10 %,)	3.4±0.5	3.1±0.4	0	6 (20 %)	0
Difference		*P*=0.009	*P*=0.015	*P*=0.027	*P*=0.031	*P*=0	*P*=0.016	*P*=0.036

chyloma or the meshwork was established ($P<0.05$). No relationships between the leak of the thoracic duct and other parameters such as the volume of pleural effusion and diameters of the thoracic duct were found in patients ($P>0.05$).

Clinical management

The triglyceride level was higher than 4.52 mmol/l in all patients, and the presence of chylomicrons appeared in six patients. Table 2 shows the position and the quantity of the chylous fluid according to the ultrasound results of the detection and measurement before percutaneous thoracic drainage. We did not find any relationships between the pleural effusion and other evaluated parameters, such as aetiology, leak of the duct, meshworks of the tiny lymphatics, thoracic duct, and chyloma ($P>0.05$). Based on the visualisation of the leak site of the thoracic duct on the continuous images, a surgical intervention was performed that proved the existence and position of the leak near the lower portion of the thoracic duct. We also found chylomas near this area in one patient. In another patient, no leak or chyloma was observed on the images, which is consistent with the surgical findings. The results were demonstrated well in two patients by ligation of the thoracic duct. In other patients, no invasive procedure was attempted because the clinical and biochemical parameters remained stable. Two patients with lymphangiomyomatosis and with less bilateral pleural fluid remained in good condition without treatment, and a 2-year follow-up showed that there was no change in the clinical and radiological conditions. Conservative treatment combined with chemotherapy was administered but failed in a patient with non-Hodgkin's lymphoma. Conservative management, which usually involved 3 to 4 weeks in the other three patients, resulted in good therapeutic effect.

Discussion

Chylothorax usually develops secondary to trauma, malignancy, congenital diseases, and other uncertain underlying causes [1–3, 16, 17]. The significant loss of essential proteins, immunoglobulins, fat, vitamins, electrolytes, and water results in metabolic and immunological disorders that can be life threatening, with a mortality rate reaching 50 %, because more chyle and lymph from the lymph duct can be found in the thoracic cavity [18, 19]. Hence, the imaging findings of the chylothorax must be characterised to aid the treatment management. The traditional method of detecting the lymph duct is bipedal radiographic lymphography [6, 7]. However, the method has a low detection rate even for the cisterna chyli of about 53 % [20]. Moreover, this method has other limitations such as the need for oily contrast agents

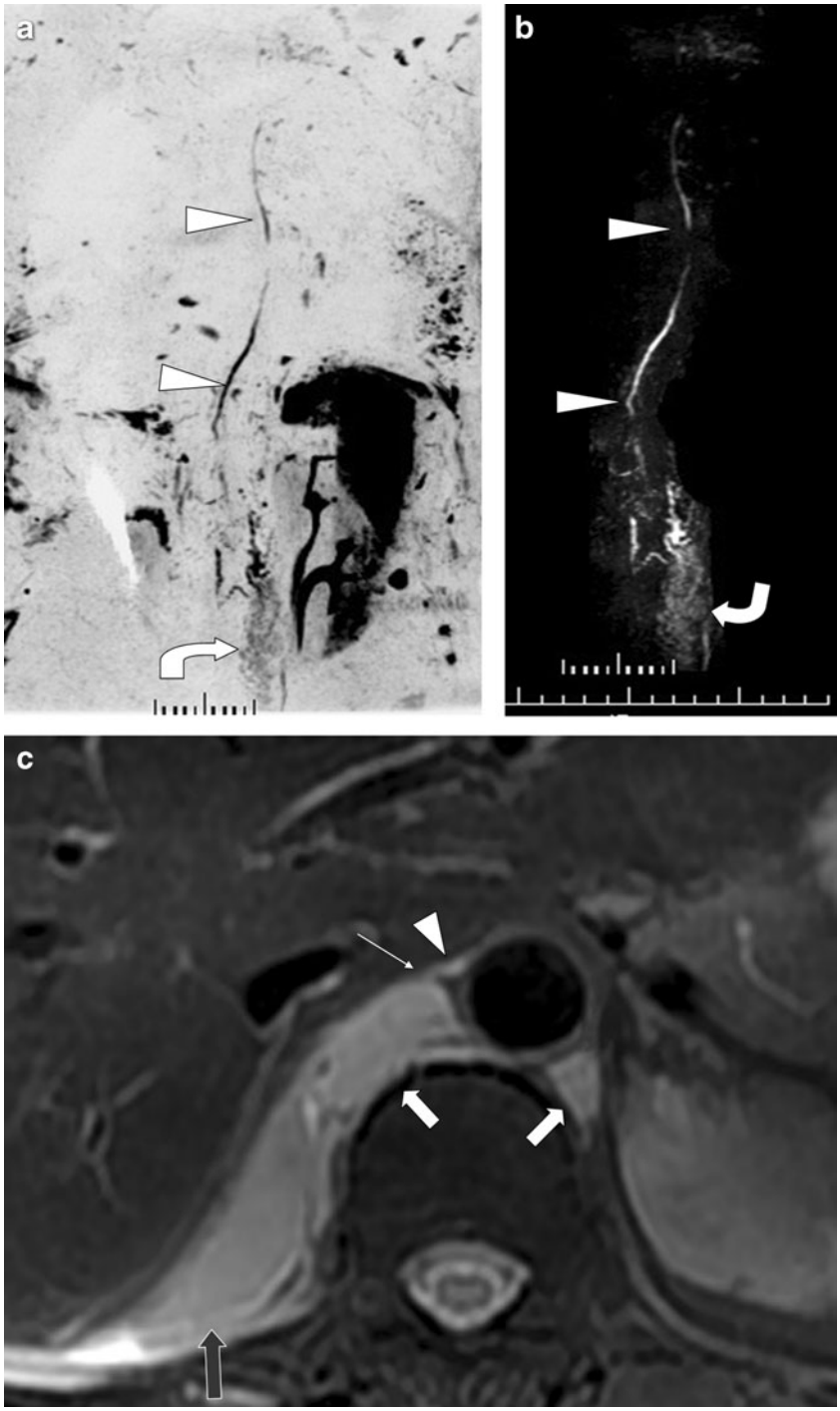

Fig. 1 A 54-year-old woman with chylothorax caused by non-Hodgkin's lymphoma. **a** MIP image shows the entire configuration of the thoracic duct (*arrowhead*) and the meshworks of tiny lymphatics (*curved arrow*) with some fluid-containing hyperintense structures of other tissues and organs. **b** The same MIP image as **a** without such fluid-containing hyperintense structures. **c** A slice of fat-saturated T2WI shows the thoracic duct (*arrowhead*), the chylomas (*wide white arrow*) on the both sides of the aorta, the leak (*thin white arrow*) between the thoracic duct and the right chyloma, and the pleural effusion on the right side (*black arrow*)

and lengthy examination [5]. Over the past few years, the highly fluid-sensitive T2WI sequences have had an important function in the visualisation of the thoracic duct and some large lymph ducts based on the sequences with a long echo time, which shows the relatively stationary fluid in the body as bright structures against a dark background [5, 8, 9]. In view of the limitations of slice thickness and the gap on the traditional axial and coronal images, the 3D MIP reconstruction of the heavily T2WI should be utilised and might allow a precise evaluation and measurement of the entire thoracic duct and accessory lymph channels. For an excellent 3D view of the thoracic duct and the accessory lymph channels, thicknesses less than 1.5 mm with no intersection gap with large matrix and a number of excitations should be used. However, this strategy might increase the scanning duration. Other high signal from fluid-containing tissues and organs should be cut out during post-processing to reduce the display interference (Fig. 1a versus b, Fig. 2a versus b).

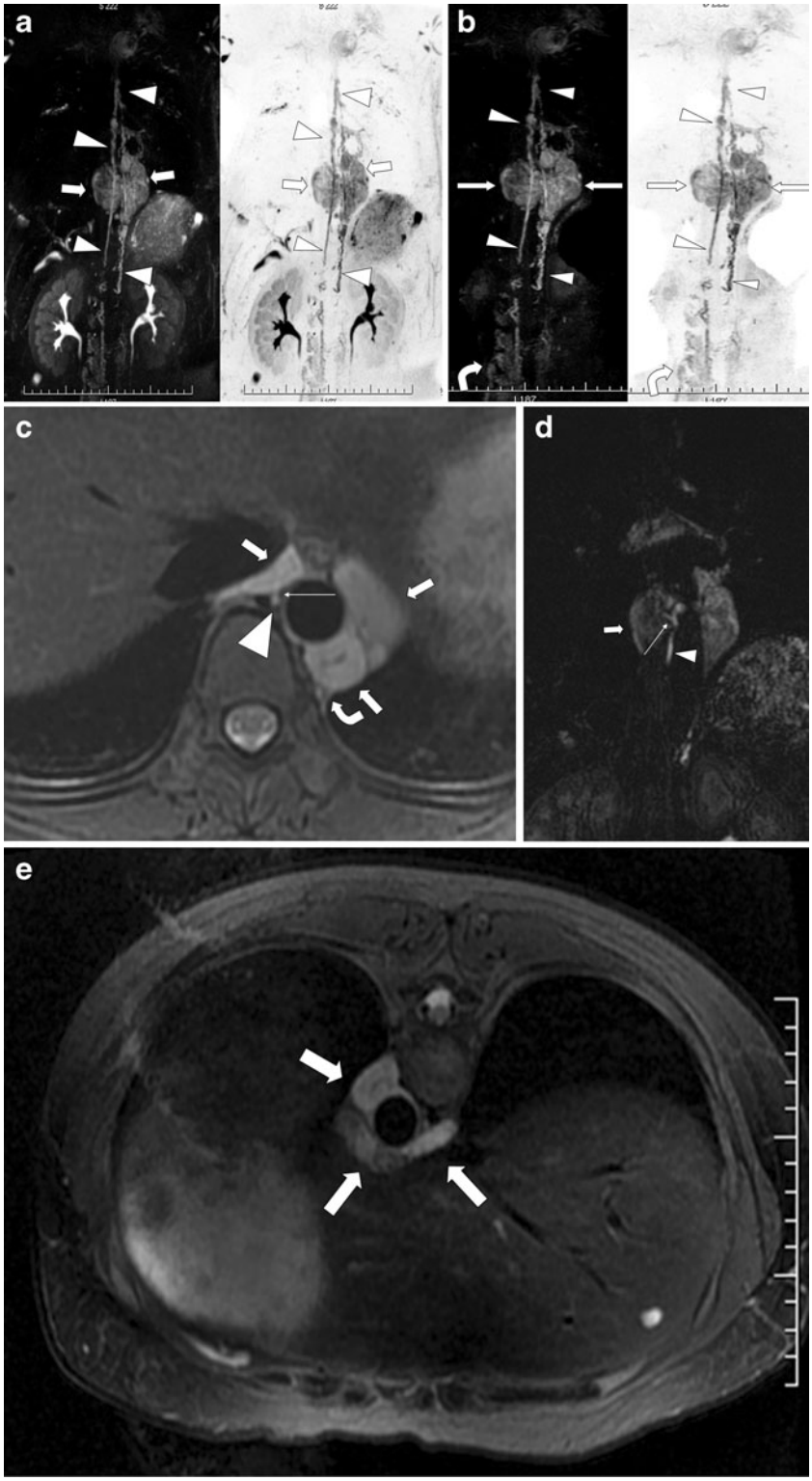

Fig. 2 A 31-year-old woman with chylothorax caused by lymphangiomyomatosis for 2 years. **a** The MIP image shows an anatomical variation of double thoracic ducts (*arrowhead*) and the imaging appearances of the chylomas (*straight wide arrow*) with other fluid-containing hyperintense structures, and then the tortuous and dilated ducts converge into one in the upper thoracic area. **b** The same MIP image as **a** without such fluid-containing hyperintense structures. **c** A slice of fat-saturated T2WI shows the thoracic duct (*arrowhead*), the chylomas (*wide white arrow*) on both sides of the aorta, the leak between the thoracic duct and the right chyloma (*thin white arrow*) and the leak of the parietal pleura from mediastinal chyloma to the pleural cavity in the left side (*curved arrow*). **d** A slice of coronal source image from the heavily T2WI shows the leak (*thin arrow*) of the thoracic duct (*arrowhead*) into the right chyloma (*wide arrow*). **e** The prone fat-saturated T2WI shows that the position of the chylomas is fixed

Higher detection rates of the thoracic duct and accessory lymph channels using the method rather than using radiograph lymphography were previously reported [5, 21]. The patients with chylothorax had several abnormal imaging findings compared with the control group in this study. Aside from a higher display rate of the entire thoracic duct and some accessory lymphatic channels in patients, our results revealed enlarged diameters and tortuous configuration of the thoracic duct and the existence of the chylomas in the posterior mediastinum.

The thoracic duct trunks are embryologically bilateral. Hence, many anatomical variations exist in more than 40 %

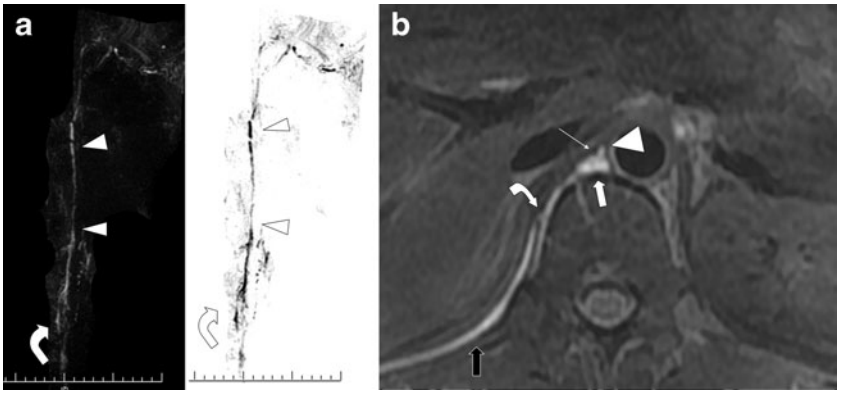

Fig. 3 A 23-year-old man with a history of trauma due to a bicycle collision, presenting with moderate volume of pleural chylous fluid in the right side. **a** The MIP image reveals the tortuous and dilated thoracic duct (*arrowhead)* and the meshworks of tiny lymphatics (*curved arrow*). **b** A slice of fat-saturated-T2WI reveals the thoracic duct (*arrowhead*), the chylomas (*wide white arrow*) on the right sides of the aorta, the leak between the thoracic duct and the right chyloma (*thin white arrow*), the leak of the parietal pleura from chyloma to the pleural cavity (*curved arrow*), and the pleural effusion on the right side (*black arrow*)

of the population [21, 22]. The bilateral ducts in two patients were also shown in the present study, which possibly indicates that anatomical variations might increase the possibility of thoracic duct injury. The visualisation of anatomical variations may avoid complications during surgery [16, 21]. Aside from the entire display and the enlarged diameters and tortuous configuration of the thoracic duct, the accessory lymph channels with a high display rate existed in two regions: the first lying along the vertebral and aortic regions in the upper abdomen and draining into the cisterna chyli via connections of small lymph channels or lymph trunks that are considered the meshworks of the tiny lymphatics according to Pinto's [23] and Erden's [8] reports, and the second in the left subclavian region, which was not found in the control group. We presume that the high display rates of the thoracic duct and the accessory lymphatic channels are probably related to the obstruction of the thoracic duct, and the obstruction in the second region may be more distal. In addition, unlike focal collections of chylous fluid, the chyloma is usually located in the posterior mediastinum, which is adjacent to the thoracic duct rather than in the pleural cavity. In this study, we showed a high display rate of the chyloma (85.7 %) in patients with chylothorax, characterised by a well-demarcated and cyst-like signal previously described in a case report of diffuse lymphangiomatosis [24]. We also found some small hyperintense channels between the chylomas, which indicated that a single leak of the thoracic duct might result in multiple chylomas via the connected lymphatic channels. Our results showed that the chylomas in two patients remained unchanged for a long period, which is possibly related to the relatively low pressure within the thoracic duct and a slower progression of the chronic disease.

Regardless of the aetiology, the accurate diagnosis and localisation of the leak site are paramount in the management of any chyle leak particularly in preoperative planning. The leak site should be determined via the thin, continuous axial and coronal images rather than the MIP images to decrease the overlap and confusion of structures near the

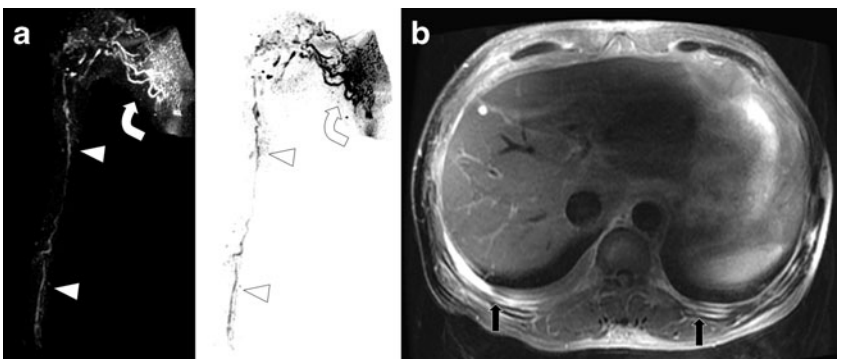

Fig. 4 A 54-year-old man involved in a high-speed road traffic accident, suffering multiple fractures of the right humerus and scapula with a moderate volume of pleural chylous fluid on the bilateral sides. **a** The MIP image reveals the torturous thoracic duct (*arrowhead*) and the torturous and dilated lymphatic channels (*curved arrow*) in the left subclavian region communicating with the upper segment of the thoracic duct. **b** Besides the bilateral pleural chylous fluid (*black arrow*), the chyloma, leak site, and meshworks of tiny lymphatics are not found on all continuous fat-saturated T2WI and source images of heavily T2WI

Table 2 The clinical features and imaging changes of the patients with chylothorax

Patient no.	Sex	Age	Clinical management	Aetiology	Chylous pleural fluid		FS-T2WI				MIP					
					Position	[a]Quantity	Number of leaks in TD	Number of leaks in parietal pleura	Number of chylomas	Chyloma location	Number of TD	TD display	Transverse diameter of TD (mm)	Anteroposterior diameter of TD (mm)	Lymphatics in left subclavian region	Meshworks of tiny lymphatics
1	F	54	Conservative	Lymphoma	Right	More	1	Overlapped	More	Bilateral	1	Entire	4.2	4.0	No	Yes
2	F	31	None	LAM	Bilateral	Less	2	1	More	Bilateral	2	Entire	6.5	6.3	No	Yes
3	F	25	Conservative	LAM	Bilateral	Less	1	1	More	Bilateral	1	Lower 2/3 portion	3.5	3.5	No	Yes
4	M	23	Conservative	Trauma	Right	Moderate	1	1	Single	Right	1	Entire	3.9	3.6	No	Yes
5	M	54	Surgical	Trauma	Bilateral	Moderate	Non	Non	Non	Non	1	Entire	3.6	3.4	Yes	No
6	F	24	Surgical	Unknown	Bilateral	Moderate	2	2	More	Bilateral	2	Lower 2/3 portion	6.5	6.3	No	Yes
7	F	58	Conservative	Unknown	Bilateral	Less	Overlapped	Overlapped	More	Bilateral	1	Entire	5.7	4.1	No	No

TD Thoracic duct; *LAM* lymphangiomyomatosis

[a] Less (≤380 ml with the effusion width ≤20 mm), moderate (380 ml–1,000 ml with the effusion width 20 mm–40 mm) and more (≥1,000 ml with the effusion width ≥40 mm), according to the maximum width of the fluid lamella along the lateral chest wall at ultrasound during maximum inspiration with the patient completely supine, presented by Eibenberger et al. [14]

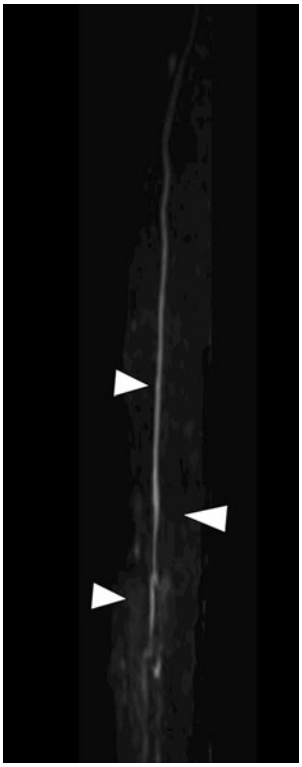

Fig. 5 A 43-year-old male healthy control. The MIP image reveals a thin and smooth thoracic duct

lymphatic duct. Our results of this study revealed seven leak sites from the thoracic duct to chyloma in five patients and five leak sites from chyloma to pleural cavity in four patients based on T2WI and the source images of the heavily T2WI. Among these patients, one with a leak of the duct and another without leakage were confirmed by both imaging and surgical observation. These results indicate that MRI may be a reliable approach to determine the location of the leakage in presurgical patients and help in coming up with an appropriate treatment plan. The observations made in this study described a follow-up of two patients with lymphangiomyomatosis, which revealed that the clinical condition and radiological findings including the pleural effusion, chyloma, and thoracic duct remained stable for 2 years. This observation demonstrates that the technique may be regarded as a potential tool for follow-up or evaluation of the therapeutic effect. Motoyama et al. [25] reported that the leakage point could be shown on axial MR images in a case report where the leakage site was indefinitely marked in the figures. As a consequence, their study did not differentiate the leak site from the enlarged duct or chyloma based on the indefinitely marked figures.

The close relationship between the leak of the thoracic duct and the chyloma was observed despite the small sample number. Therefore, the leak site of the thoracic duct should be determined at the level of the chyloma once the chyloma appeared. The neighbouring chyloma may cover or mask the leak site. For patients with chylothorax who need surgical planning but without leakage on images, the presentation of the chyloma itself is an indicator that helps determine the exact location of the leak site of the duct. Most chylomas in the present study result from some non-traumatic causes. However, a statistical conclusion was not obtained because of a small sample size. All chylomas in this study were located in the lower two-thirds of the thoracic duct, which indicates that this portion is most easily injured. In addition, the close relationship between the leak of the thoracic duct and the meshworks of the tiny lymphatics was shown, which indicates that the pressure within the thoracic duct is higher because of the distal obstruction and may promote the rupture of the duct and the dilation of the tiny lymphatics flowing into the cisterna chyli. However, relationships between the leak of the thoracic duct and other evaluated parameters were not obtained, probably because of the small sample size. Moreover, we also considered that the number of leak sites of the parietal pleura should be in accordance with the sides of the pleural effusion (right, left, or bilateral sides). In fact, most leak sites of the parietal pleura were not visualised because of the overlapping and covering of the high signals of very close pleural effusion. Fortunately, the management for chylothorax usually focuses on the leak of the thoracic duct.

The study has several limitations. Firstly, the study population with chylothorax is quite small, which may influence the interpretation of this study and the accuracy of the statistical results. Therefore, the number of patients and individuals in the control group needs to be increased. Secondly, this study pools the compared analysis with surgical or other imaging results. In addition, some small leak points may be overlapped or covered by nearby pleural fluid, chyloma, and dilated lymphatics because some structures with high signal had an impact on the leakage of the thoracic duct. The tiny leak point may also be omitted because of the limited resolution of the MRI as of this writing. Hence, the combination of the fluid-sensitive sequence with another imaging technique may increase the visualised and identified accuracy of the leak site. Further investigations are needed to overcome these shortcomings.

In conclusion, these cases highlight the ability of T2WI and 3D MIP sequences to illustrate the leak site and chyloma and to display the dilated and tortuous configuration of the thoracic duct and accessory lymphatic channels in patients with chylothorax. When no leak site has been confirmed, the site of chyloma may be a helpful indicator to find the leak site nearby. As a safe, non-invasive, and simple technique, unenhanced MRI appears to be a reliable and suitable approach in the visualisation of the abnormal thoracic duct and accessory lymphatic channels, which helps in determining an appropriate treatment plan and a follow-up for evaluating the therapeutic effect for patients with chylothorax.

References

1. McGrath EE, Blades Z, Anderson PB (2010) Chylothorax: aetiology, diagnosis and therapeutic options. Respir Med 104:1–8
2. Talwar A, Lee HJ (2008) A contemporary review of chylothorax. Indian J Chest Dis Allied Sci 50:343–351
3. Smoke A, Delegge MH (2008) Chyle leaks: consensus on management? Nutr Clin Pract 23:529–532
4. Restrepo CS, Eraso A, Ocazionez D, Lemos J, Martinez S, Lemos DF (2008) The diaphragmatic crura and retrocrural space: normal imaging appearance, variants, and pathologic conditions. Radiographics 28:1289–1305
5. Hayashi S, Miyazaki M (1999) Thoracic duct: visualization at nonenhanced MR lymphography–initial experience. Radiology 212:598–600
6. Kos S, Haueisen H, Lachmund U, Roeren T (2007) Lymphangiography: forgotten tool or rising star in the diagnosis and therapy of postoperative lymphatic vessel leakage. Cardiovasc Intervent Radiol 30:968–973
7. Deso S, Ludwig B, Kabutey NK, Kim D, Guermazi A (2012) Lymphangiography in the diagnosis and localization of various chyle leaks. Cardiovasc Intervent Radiol 35:117–126
8. Erden A, Fitoz S, Yagmurlu B, Erden I (2005) Abdominal confluence of lymph trunks: detectability and morphology on heavily T2-weighted images. AJR Am J Roentgenol 184:35–40
9. Takahashi H, Kuboyama S, Abe H, Aoki T, Miyazaki M, Nakata H (2003) Clinical feasibility of noncontrast-enhanced magnetic resonance lymphography of the thoracic duct. Chest 124:2136–2142
10. Matsushima S, Ichiba N, Hayashi D, Fukuda K (2007) Nonenhanced magnetic resonance lymphoductography: visualization of lymphatic system of the trunk on 3-dimensional heavily T2-weighted image with 2-dimensional prospective acquisition and correction. J Comput Assist Tomogr 31:299–302
11. Okuda I, Udagawa H, Takahashi J, Yamase H, Kohno T, Nakajima Y (2009) Magnetic resonance-thoracic ductography: imaging aid for thoracic surgery and thoracic duct depiction based on embryological considerations. Gen Thorac Cardiovasc Surg 57:640–646
12. Kato T, Takase K, Ichikawa H, Satomi S, Takahashi S (2011) Thoracic duct visualization: combined use of multidetector-row computed tomography and magnetic resonance imaging. J Comput Assist Tomogr 35:260–265
13. Yu DX, Ma XX, Zhang XM, Wang Q, Li CF (2010) Morphological features and clinical feasibility of thoracic duct: detection with nonenhanced magnetic resonance imaging at 3.0 T. J Magn Reson Imaging 32:94–100
14. Eibenberger KL, Dock WI, Ammann ME, Dorffner R, Hörmann MF, Grabenwöger F (1994) Quantification of pleural effusions: sonography versus radiography. Radiology 191:681–684
15. Doerr CH, Miller DL, Ryu JH (2001) Chylothorax. Semin Respir Crit Care Med 22:617–626
16. Akcali O, Kiray A, Ergur I, Tetik S, Alici E (2006) Thoracic duct variations may complicate the anterior spine procedures. Eur Spine J 15:1347–1351
17. Doerr CH, Allen MS, Nichols FC 3rd, Ryu JH (2005) Etiology of chylothorax in 203 patients. Mayo Clin Proc 80:867–870
18. Nair SK, Petko M, Hayward MP (2007) Aetiology and management of chylothorax in adults. Eur J Cardiothorac Surg 32:362–369
19. Denk PM, Gatta P, Swanström LL (2008) Multimedia article. Prone thoracoscopic thoracic duct ligation for postsurgical chylothorax. Surg Endosc 22:2742
20. Verma SK, Mitchell DG, Bergin D et al (2009) Dilated cisternae chyli: a sign of uncompensated cirrhosis at MR imaging. Abdom Imaging 34:211–216
21. Erden A (2004) Cisterna chyli: an incidental finding on MR cholangiopancreatography. AJR Am J Roentgenol 82:262
22. Liu ME, Branstetter BF 4th, Whetstone J, Escott EJ (2006) Normal CT appearance of the distal thoracic duct. AJR Am J Roentgenol 18:1615–1620
23. Pinto PS, Sirlin CB, Andrade-Barreto OA, Brown MA, Mindelzun RE, Mattrey RF (2004) Cisterna chyli at routine abdominal MR imaging: a normal anatomic structure in the retrocrural space. Radiographics 4:809–817
24. Ozturk A, Yousem DM (2007) Magnetic resonance imaging findings in diffuse lymphangiomatosis: neuroradiological manifestations. Acta Radiol 48:560–564
25. Motoyama S, Okuyama M, Saito R, Kitamura M, Ishiyama K, Ogawa J (2005) Magnetic resonance imaging for chylothorax after esophagectomy. Jpn J Thorac Cardiovasc Surg 53:434–436